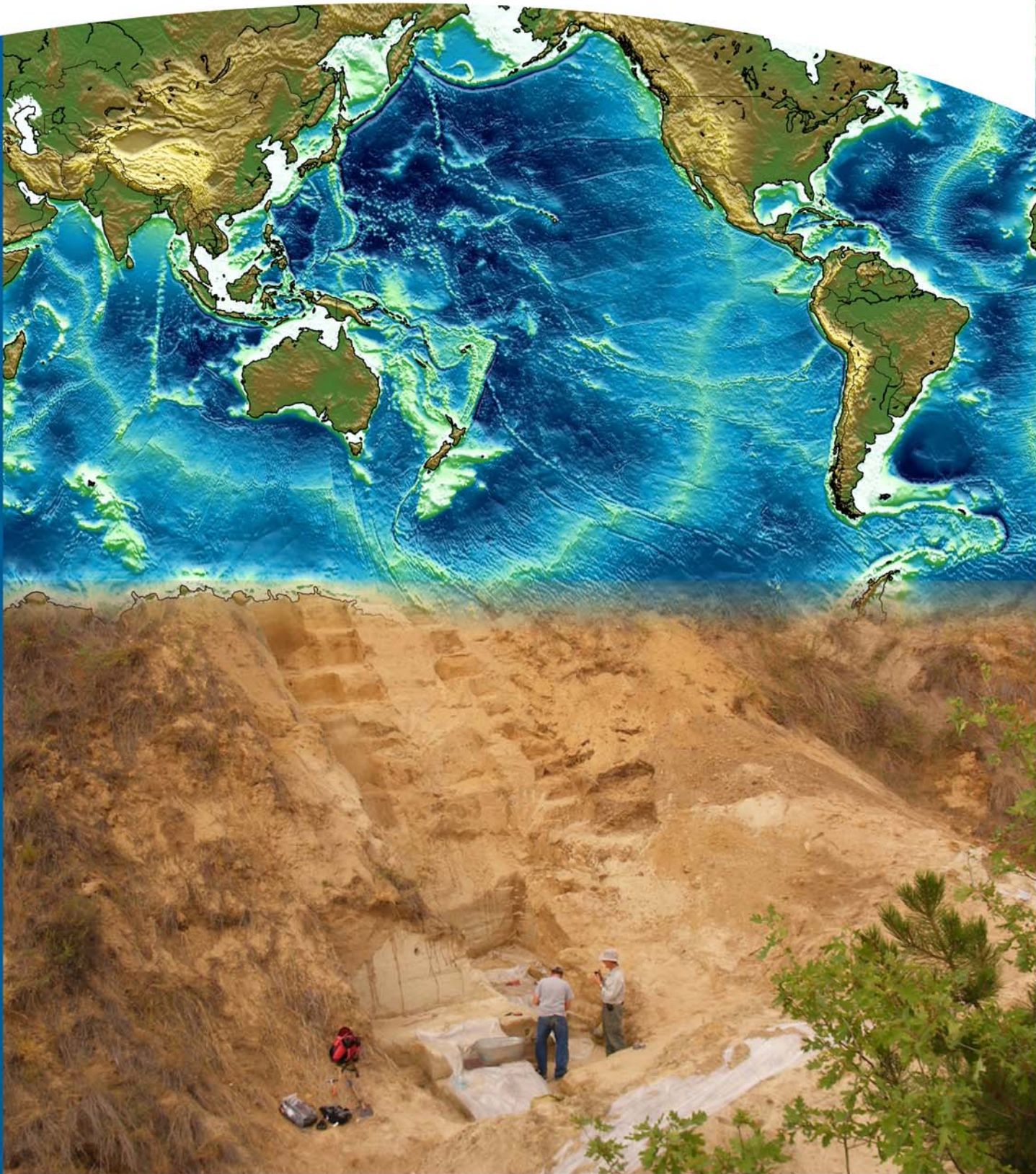


ISSN : 2395-647X

Vol. 2, No. 1, March 2016



International Journal of Geology and Earth Sciences



www.ijges.com

Email : info.ijges@gmail.com or editor@ijges.com

Research Paper

MAJOR AND TRACE ELEMENT CHEMISTRY OF CHROMIAN SPINELS IN PERIDOTITES FROM YESILOVA OPHIOLITE (SW TURKEY): PETROGENETIC INTERPRETATION

Özgür Bilici^{1*} and Hasan Kolaylı²*Corresponding Author: **Özgür Bilici** ✉ ozgurbilici@atauni.edu.tr

The Yesilova ophiolite is one of the most important tectonic unit represented the western part of the ophiolite belts of the Anatolide-Tauride block, SW Turkey. In this study, we discussed the harzburgite-dunite suite in the mantle sequence of this ophiolite using the mineral chemistry of the chromian spinels. On the basis of the Cr# and Mg# values, the spinels in the harzburgite and dunite are similar to those from fore-arc peridotites. The relatively high-Cr# and low-Ti contents of the chromian spinels in the harzburgite signify that they belong to a supra-subduction setting. However, the Cr#-TiO₂ relationships in the chromian spinels from the dunite favor a melt-rock interaction model in which dunite with relatively high-Al and high-Ti spinels were produced by the interaction of harzburgite with MORB-like melt. Also, this study uses Laser Ablation–Inductively Coupled Plasma–Mass Spectrometry (LA–ICP–MS) to better understand the relationship between the harzburgite and dunite based on the chromian spinel chemistry. The trace element concentrations of the spinels show that Ga, Ni, V, Zn, Co contents decrease, and Sc, Ti, Mn and LREE contents increase from the harzburgite to the dunite, suggesting a control by partial melting, and all studied chromian spinels reveal a subduction zone environment.

Keywords: Chromian spinel, Peridotite, Subduction zone, Yesilova ophiolite

INTRODUCTION

Chromian spinel has been commonly used as a petrogenetic indicator in the mantle peridotites of many ophiolites and other magmatic environments (Irvine, 1965, 1967; Jackson, 1969; Hill and Roeder, 1974; Sack and Ghiorso, 1991; Arai, 1992, 1994; Roeder, 1994; Barnes and Roeder, 2001; Kamenetsky *et al.*, 2001; Arai *et al.*, 2011) because its chemical composition

depends on the degree of fractional crystallization of the parental melt and the degree of partial melting experienced by the mantle source (Maurel and Maurel, 1982; Kamenetsky *et al.*, 2001; Dick and Bullen, 1984; Arai, 1994; Roeder, 1994; Barnes and Roeder, 2001; González-Jiménez *et al.*, 2013, 2015). Therefore, the chromian spinels in the peridotites are used for petrotextonic discrimination between Mid-Ocean

¹ Department of Geological Engineering, Ataturk University, Erzurum, Turkey.

² Department of Geological Engineering, Karadeniz Technical University, Trabzon, Turkey.

Ridge (MOR) and supra-subduction zone (SSZ) settings (Dick and Bullen, 1984; Parkinson and Pearce, 1998; Pearce *et al.*, 2000; Arai *et al.*, 2006; Shi *et al.*, 2012). In addition, the Cr# of the chromian spinel with the Mg# is high variable and uses as a critical indicator for ultramafic and related rocks (Irvine, 1967; Dick and Bullen, 1984). Plutonic rocks have relatively low-Ti spinels from the supra-subduction setting, and according to spinel chemistry, the dunites are almost indistinguishable from the harzburgites (e.g., Arai, 1994; Arai *et al.*, 2011).

Many researchers indicate that the mineralogical and the geochemical characteristics of the peridotites in ophiolites are also an important source of information about the melt evolution, petrological processes and dynamics of the upper mantle in different tectonic environments (e.g., Parkinson and Pearce, 1998; Flower and Dilek, 2003; Uysal *et al.*, 2007, 2012, 2014; Seyler *et al.*, 2007; Choi *et al.*, 2008; Moghadam *et al.*, 2015). General concensus on many peridotite massifs containing economically important chromitite orebodies are interpreted to be Supra-Subduction Zone type (SSZ), whereas chromitite-free peridotites are attributed to MOR-type abyssal in origin (Edwards *et al.*, 2000).

A suit of trace elements in chromian spinels such as Ga, Ti, Ni, Zn, Co, Mn, V and Sc provide useful information about the peridotites and the chromitites (e.g., Dare *et al.*, 2009; Pagé and Barnes, 2009; González-Jiménez *et al.*, 2011, 2013, 2014; Aldanmaz, 2012; Zhou *et al.*, 2014). These trace elements and also rare earth elements data for chromian spinels in the studied peridotites from the Yesilova ophiolite are also presented in order to investigate the relationship between the harzburgite and the dunite.

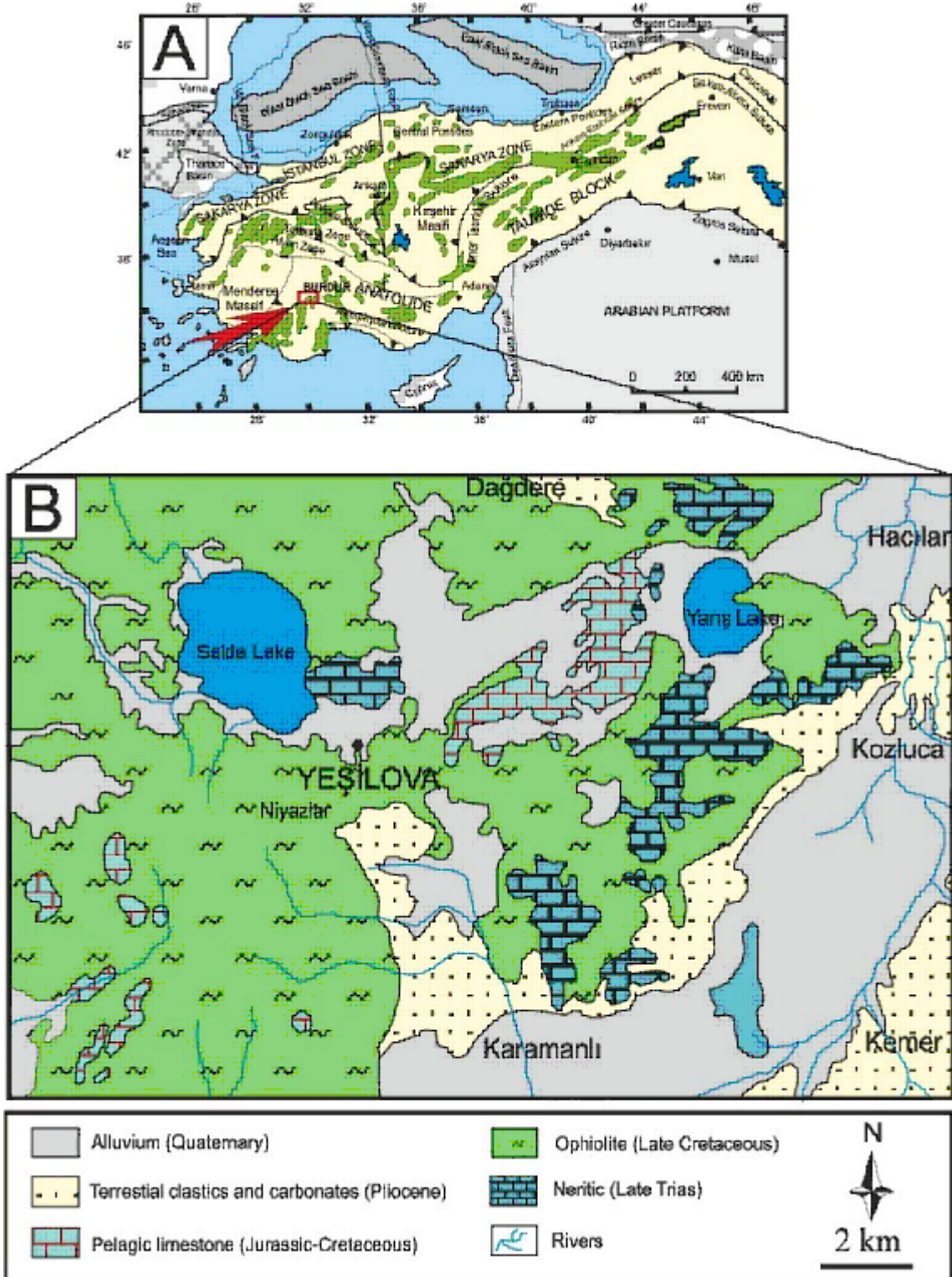
Here, we studied harzburgite-dunite suite in the mantle sequence of the Yesilova ophiolite (SW Turkey). The main objective of this study is to report the new geochemical data of the chromian spinels in the peridotites, especially in the dunites with high-Al and relatively high-Ti chromian spinels. We emphasize that the dunite occurrence is associated with intermediate degree partial melting (~ % 25) of the harzburgite in a supra-subduction zone setting. Moreover, this study is the first to description on Rare Earth Element (REE), High-Field Strength Element (HFSE), and some transition element concentrations from in situ analysis of chromian spinels from the peridotite section of the Yesilova ophiolite, analysed by Laser Ablation–Inductively Coupled Plasma–Mass Spectrometry (LA–ICP–MS).

GEOLOGICAL SETTING

The ophiolitic rocks of Turkey are the remnants of Tethyan ophiolites in the Anatolian section of the Alpine–Himalayan Orogenic Belt. These ophiolitic rocks are found in tectonic units of Turkey composed of Pontides, Anatolides, Taurides and the Border folds (Okay and Tüysüz, 1999) (Figure 1a).

The Yesilova ophiolite (Sarp, 1976) represent the western part of the ophiolite belts of the Anatolide-Taurides, SW Turkey (Figure 1a). In the previous studies, the oldest unit in the region consists of Late Triassic neritic limestones. Jura-Cretaceous pelagic limestones and ophiolitic unit consisting of harzburgite, dunite and some sub-volcanic rocks (dolerite) are exposed on this unit. Quaternary alluvium and Pliocene age mixed unit comes on top of this unit (MTA, 2002) (Figure 1b). The lithological units are consist of Late Jurassic – Early Createaous aged Yesilova ophiolites,

Figure 1: (a) Distribution of ophiolite belts in Turkey (modified from MTA, 2002 and Okay and Tüysüz, 1999), (b) Geological map of the Yesilova region (Burdur, SW Turkey)



Upper Cenonian aged Kızılcadağ ophiolitic melange, Pliyo-Quaternary aged Niyazlar Formation and Quaternary aged alluvions in the study area (Döyen, 1995; Döyen *et al.*, 2014).

The absence of the characteristic components of the ophiolites, such as gabbro, pillow basalt and sheeted dykes suggests that the ultramafic suites in Yesilova ophiolite are at best fragments of highly tectonized and dismembered ophiolitic sequences (Döyen *et al.*, 2014).

The ultramafic rocks of the Yesilova ophiolite are mainly composed of harzburgite cutting by several diabasic dykes, and also less dunite including chromitite bodies; pyroxenites are very rare and cut dunite bodies as veins or small dykes (Bilici, 2015). However, in this investigation, we discussed only the mineralogical and petrological characteristics of the harzburgite and dunite bodies based on the spinel chemistry.

ANALYTICAL METHODS

Representative samples were collected from the harzburgites and the dunites. A series of thin sections were examined under polarizing microscope to determine the common textural and mineralogical properties of the rock varieties. The major oxide analyses of the chromian spinels were carried out on polished thin sections at the Electron Microprobe Laboratory of Maine University (USA). All elements were analyzed by Energy-Dispersive X-ray spectroscopy (EDX) using EDS and WDS detectors attached to a JEOL JSM-6300 scanning electron microscope. The accelerating voltage was 15 kV, and the beam current was 3.3 nA with a 4-mm beam diameter. The detection limits were ~0.1%, and accuracy was better than 5%. Cationic ratios were calculated on the basis of 32 oxygen atoms assuming spinel stoichiometry.

On the other hand, trace element concentrations of the chromian spinels were determined in situ for individual mineral phases using the LA-ICP-MS at Houston University (USA). The system incorporates a 193 nm Ar-F Excimer laser ablation system and a quadrupole ICP-MS with collision and reaction cell in pulse counting mode. Ablation was performed at a fixed point on the sample surface at a fluence of 20 Jcm⁻², a pulse repetition rate of 10 Hz and a typical crater diameter of 60–120 microns.

RESULTS

Field Observation and Petrography

We investigated the mantle section of the Yesilova ophiolite in this study. Field observations suggest that the harzburgitic peridotites are the most widespread lithological unit in the studied area. Less dunite zones are located within the harzburgites. These dunitic levels are separated from the harzburgites likely in the form of possible boundaries due to intermittent outcrops, and also, their locally but intensive serpentinization and gradual changes of the mineralogical composition were determined by petrographic studies (Figure 2).

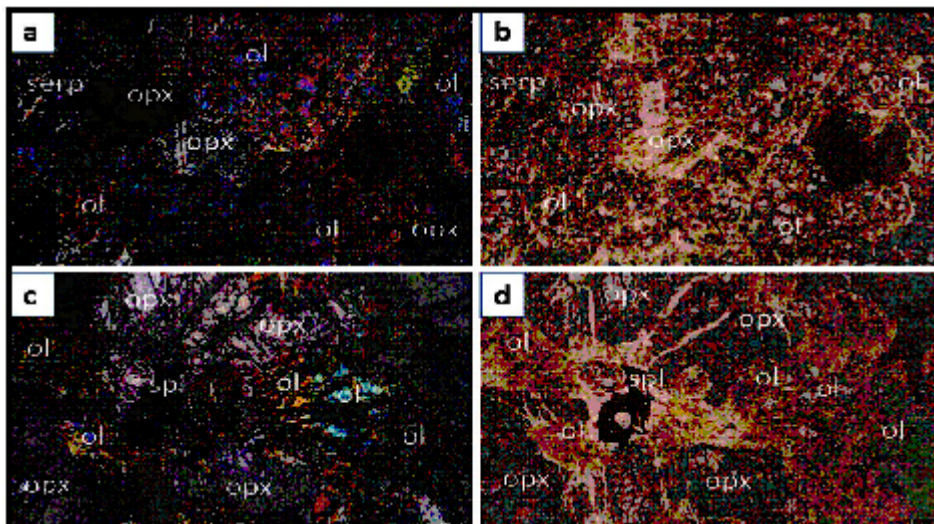
The studied harzburgites usually exhibit protogranular to weakly porphyroclastic textures, and are sometimes cataclastic to mylonitic at the contact zones. The main minerals are olivine, orthopyroxene clinopyroxene and chromian spinel. Chromian spinel (modal abundance; ~ 2 %) in the harzburgite is frequently vermicular and intergrown with olivine and orthopyroxene (Figure 3). Spinel grains are dark red to opaque and generally small and some contain silicate inclusions such as olivine (Figure 3d).

The studied dunites have generally an equigranular texture. Cataclastic to mylonitic

Figure 2: Field Photograph of the Studied Peridotites from the Yeşilova Ophiolite Possible Boundary Between the Harzburgite and Dunite Including Chromitite Mine



Figure 3: Mineralogical features of harzburgite from Yesilova ophiolite. a-c: crossed nicol, b-d: plane polarized light (ol: olivine, opx: orthopyroxene, serp: serpentine, spl: chromian spinel, olivine has been partially altered into serpentine)



textures sometimes occur at the contact zones with harzburgites. The basic minerals are olivine and chromian spinel. Most olivines are replaced by serpentine and rarely by chlorite and weakly kinked. Chromian spinels are frequently euhedral to subhedral grains (Figure 4). Dunite with 10 to 20% of chromian spinel is called spinel rich dunite in this study. Chromian spinels are dark red to opaque, and has a variety of habits and grain sizes (Figure 4b-d).

MINERAL CHEMISTRY OF CHROMIAN SPINEL

The samples analyzed in this study, normally preserve unaltered chromian spinel grains or unaltered cores. Only the analyses performed on the unaltered chromian spinels have been considered in the interpretation of the igneous petrogenesis. The representative major oxide and trace element analyses of the chromian spinels are shown in Table 1.

The Cr_2O_3 content of the spinels varies widely from 42.75 to 45.44 wt.% in harzburgite, 35.85 to 45.12 wt.% in dunite. The TiO_2 content of these grains in harzburgite and dunite varies between 0.01-0.07 wt.%, 0.13-0.42 wt.%, respectively. Also, the Al_2O_3 contents range between 23.21-26.90 wt.% in harzburgite and 21.85-25.11 wt.% in dunite. The variations in cationic ratios and oxides such as Mg# ($=\text{Mg}/(\text{Mg}+\text{Fe}^{2+})$) and Cr# ($=\text{Cr}/(\text{Cr}+\text{Al})$) along with the TiO_2 contents of the chromian spinels and Fo contents of the olivines in the harzburgite and the dunite from the Yesilova ophiolites are illustrated in Figures 5 to 7.

The studies harzburgite and dunite include relatively Al-rich chromian spinels with almost similar chemical compositions in terms of major oxide contents, interestingly. The spinels from the harzburgite and dunite plot within the fore-arc peridotites field (Figure 5). Partial melting degrees of the peridotites, both of the harzburgites and dunites, are intermediate, approximately % 25.

Figure 4: Mineralogical features of dunite from Yesilova ophiolite.
a-c: crossed nicol, b-d: plane polarized light (ol: olivine, serp: serpentine, spl: chromian spinel, olivine has been partially altered into serpentine)

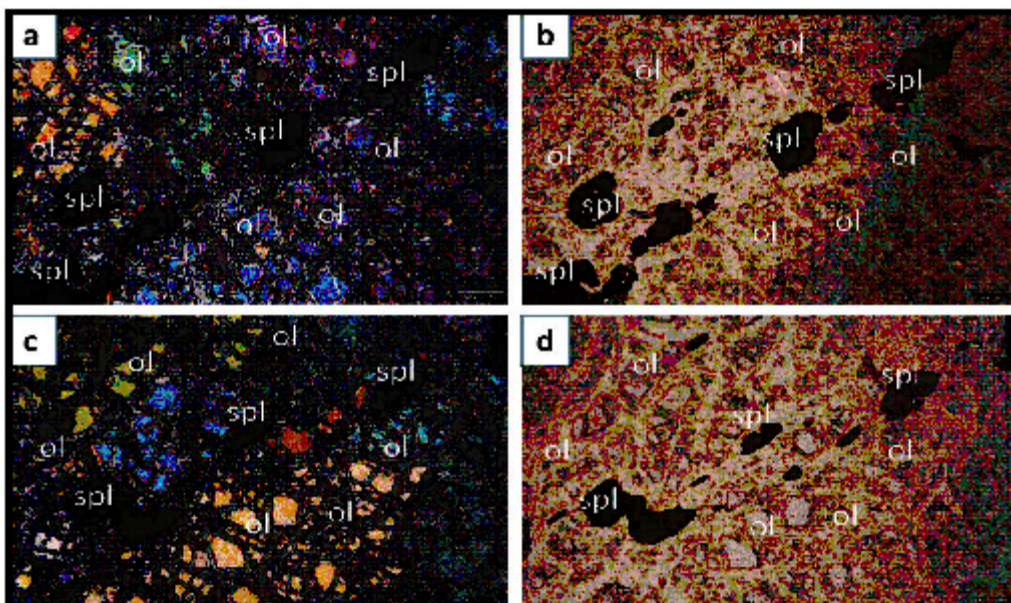


Table 1: Representative Major (Wt %) And Trace (Ppm) Element Analysis (Empa And La-icp-ms) Of The Chromian Spinel From The Yesilova Ophiolite (Sw Turkey)

Sample	MEV-1	MEV-1	MEV-1	MEV-3	MA-4	MEV-9	MEV-9	MEV-9	MEV-13	MEV-3	MEV-4	MEV-4	MEV-7	MEV-7	MEV-7	MEV-33	MEV-33	MEV-33	MEV-33
Rock-type	Wt.	Wt.	Wt.	Wt.	Wt.	Wt.	Wt.	Wt.	Wt.	Wt.									
SiO ₂	0.20	0.20	0.20	0.20	0.20	0.42	0.00	0.00	0.00	0.00	0.00	0.04	0.00	0.00	0.00	0.00	0.00	0.00	0.00
TiO ₂	0.11	0.11	0.06	0.06	0.02	0.00	0.00	0.00	0.00	0.00	0.00	0.00	0.00	0.00	0.00	0.00	0.00	0.00	0.00
Al ₂ O ₃	25.48	25.32	25.78	26.88	25.07	21.71	24.88	23.21	28.80	24.27	23.88	23.88	24.25	24.20	24.20	23.11	22.72	22.08	23.88
Cr ₂ O ₃	44.28	44.22	43.60	44.87	45.44	40.66	43.11	42.24	42.53	42.89	43.82	43.88	43.27	42.42	41.45	39.69	37.27	27.08	28.88
FeO	17.18	17.00	17.08	17.08	17.08	16.79	16.79	16.42	16.81	16.87	17.98	17.28	16.85	16.15	16.04	21.02	20.80	20.28	21.74
MnO	0.26	0.20	0.24	0.26	0.20	0.27	0.31	0.24	0.26	0.31	0.25	0.23	0.24	0.26	0.21	0.15	0.17	0.24	0.28
MgO	13.14	13.18	13.00	13.29	13.08	13.88	13.21	13.28	13.53	13.42	14.88	14.82	14.21	13.82	14.48	10.48	10.28	10.88	10.88
CaO	0.11	0.11	0.11	0.10	0.10	0.10	0.10	0.10	0.10	0.10	0.10	0.10	0.10	0.10	0.10	0.10	0.10	0.10	0.10
Total	100.20	100.25	100.25	99.98	100.27	94.12	100.25	97.23	100.13	100.28	97.25	97.24	100.28	100.71	100.93	94.48	92.84	92.77	92.24
Cr	8.49	8.32	8.44	8.70	8.73	8.89	8.89	8.68	8.15	8.18	8.28	8.14	8.17	8.20	7.96	8.24	8.45	8.01	7.52
Fe ²⁺	3.20	3.19	3.25	3.27	3.27	3.46	3.18	3.20	3.11	3.20	3.29	3.20	3.24	3.08	3.04	4.61	4.60	4.72	3.80
Fe ³⁺	0.27	0.28	0.21	0.14	0.10	0.18	0.25	0.24	0.24	0.28	0.14	0.19	0.28	0.21	0.28	0.24	0.24	0.24	0.24
Cr#	0.24	0.24	0.23	0.23	0.23	0.24	0.23	0.23	0.23	0.24	0.24	0.23	0.24	0.24	0.23	0.23	0.23	0.23	0.23
Mg#	0.60	0.60	0.59	0.58	0.58	0.57	0.60	0.60	0.60	0.60	0.60	0.60	0.60	0.60	0.60	0.57	0.52	0.54	0.52
Sc	43.60	43.38	43.45	43.58	43.44	43.28	43.28	43.28	43.28	43.28	43.28	43.28	43.28	43.28	43.28	43.28	43.28	43.28	43.28
Ti	236.81	237.89	232.29	237.89	232.81	232.89	234.89	241.24	232.42	189.87	189.53	187.82	189.17	187.89	185.58	188.87	187.82	187.82	187.82
Y	0.54	0.52	0.42	0.50	0.50	0.29	0.30	0.32	0.32	0.08	0.08	0.08	0.07	0.08	0.08	0.08	0.08	0.08	0.07
Co	1028.12	934.24	1012.12	934.82	873.82	912.88	938.48	928.47	981.88	184.74	182.57	182.51	188.88	184.82	182.27	184.74	182.27	182.21	182.48
Ni	8955.84	1887.84	8981.24	1227.51	1159.94	1488.28	1172.80	1182.24	1291.86	1274.20	894.28	893.11	894.84	892.28	817.73	1275.29	894.28	893.21	893.84
Zn	3762.84	3784.45	3879.28	3824.49	3445.29	2888.21	2882.89	2822.18	4322.86	274.79	281.01	280.91	280.82	280.29	280.22	274.79	280.21	280.81	280.49
Ga	57.28	58.02	58.02	63.20	58.29	64.27	58.23	57.84	58.23	26.25	28.27	27.42	25.83	27.78	26.02	26.23	26.23	26.27	27.42
Mo	0.22	0.24	0.18	0.14	0.18	0.14	0.14	0.14	0.14	0.09	0.09	0.09	0.09	0.09	0.09	0.09	0.09	0.09	0.09
Rb	8.47	4.78	1.87	0.47	0.78	0.77	0.29	0.08	2.87	2.02	1.18	0.27	0.27	0.11	0.04	2.62	1.18	0.27	0.27
Y	0.20	0.22	0.22	0.22	0.21	0.07	0.02	0.02	0.04	0.08	0.02	0.08	0.08	0.01	0.02	0.02	0.02	0.02	0.02
Zr	0.99	0.82	0.80	0.84	0.82	0.29	0.61	0.25	0.28	0.12	0.12	0.12	0.14	0.12	0.12	0.12	0.12	0.12	0.12
Nb	0.61	0.71	0.69	0.76	0.78	0.70	0.78	0.86	0.79	0.14	0.12	0.12	0.12	0.12	0.12	0.12	0.12	0.12	0.12
Ca	0.29	0.31	0.30	0.31	0.30	0.12	0.01	0.01	0.01	0.01	0.01	0.01	0.01	0.01	0.01	0.01	0.01	0.01	0.01
Ba	2.25	4.78	1.98	1.92	2.28	3.10	0.24	0.07	7.18	0.08	0.44	0.12	0.24	0.03	0.01	0.80	0.40	0.11	0.24
La	0.82	0.80	0.81	0.81	0.81	0.80	0.80	0.80	0.80	0.80	0.80	0.80	0.80	0.80	0.80	0.80	0.80	0.80	0.80
Ce	0.28	0.28	0.28	0.28	0.28	0.28	0.28	0.28	0.28	0.28	0.28	0.28	0.28	0.28	0.28	0.28	0.28	0.28	0.28
Pr	0.11	0.10	0.11	0.10	0.11	0.10	0.10	0.10	0.10	0.10	0.10	0.10	0.10	0.10	0.10	0.10	0.10	0.10	0.10
Nd	0.25	0.23	0.23	0.23	0.23	0.23	0.23	0.23	0.23	0.23	0.23	0.23	0.23	0.23	0.23	0.23	0.23	0.23	0.23
Sm	0.08	0.08	0.08	0.08	0.08	0.08	0.08	0.08	0.08	0.08	0.08	0.08	0.08	0.08	0.08	0.08	0.08	0.08	0.08
Eu	0.22	0.21	0.20	0.21	0.21	0.21	0.21	0.21	0.21	0.21	0.21	0.21	0.21	0.21	0.21	0.21	0.21	0.21	0.21
Gd	0.23	0.24	0.22	0.22	0.24	0.22	0.22	0.22	0.22	0.22	0.22	0.22	0.22	0.22	0.22	0.22	0.22	0.22	0.22
Tb	0.10	0.11	0.11	0.10	0.10	0.10	0.10	0.10	0.10	0.10	0.10	0.10	0.10	0.10	0.10	0.10	0.10	0.10	0.10
Dy	0.25	0.24	0.25	0.25	0.25	0.25	0.25	0.25	0.25	0.25	0.25	0.25	0.25	0.25	0.25	0.25	0.25	0.25	0.25
Ho	0.11	0.10	0.11	0.11	0.10	0.10	0.10	0.10	0.10	0.10	0.10	0.10	0.10	0.10	0.10	0.10	0.10	0.10	0.10
Er	0.08	0.02	0.04	0.02	0.02	0.01	0.02	0.02	0.02	0.02	0.02	0.02	0.02	0.02	0.02	0.02	0.02	0.02	0.02
Tm	0.11	0.11	0.11	0.11	0.11	0.11	0.11	0.11	0.11	0.11	0.11	0.11	0.11	0.11	0.11	0.11	0.11	0.11	0.11
Yb	0.24	0.24	0.27	0.23	0.24	0.24	0.24	0.24	0.24	0.24	0.24	0.24	0.24	0.24	0.24	0.24	0.24	0.24	0.24
Lu	0.11	0.10	0.11	0.11	0.11	0.11	0.11	0.11	0.11	0.11	0.11	0.11	0.11	0.11	0.11	0.11	0.11	0.11	0.11
ΣRE	0.84	0.83	0.84	0.82	0.82	0.81	0.81	0.81	0.81	0.81	0.81	0.81	0.81	0.81	0.81	0.81	0.81	0.81	0.81
Th	0.11	0.10	0.11	0.11	0.11	0.11	0.11	0.11	0.11	0.11	0.11	0.11	0.11	0.11	0.11	0.11	0.11	0.11	0.11
Pb	0.25	0.24	0.27	0.23	0.24	0.24	0.24	0.24	0.24	0.24	0.24	0.24	0.24	0.24	0.24	0.24	0.24	0.24	0.24
U	0.12	0.12	0.12	0.12	0.12	0.12	0.12	0.12	0.12	0.12	0.12	0.12	0.12	0.12	0.12	0.12	0.12	0.12	0.12
Σ	8.89	8.89	8.89	8.89	8.89	8.89	8.89	8.89	8.89	8.89	8.89	8.89	8.89	8.89	8.89	8.89	8.89	8.89	8.89

The chromian spinels in the harzburgite show high Cr# (~0.52 to 0.56) along with low TiO₂ (<0.15%) (Figure 7). The Cr# of these spinels is commonly higher than those of typical MOR spinels, and could be a residue after high degrees of partial melting of the mantle peridotites. Some of the spinels in the dunites are generally characterized by relatively higher Cr#, and show similar TiO₂ abundance. However, most of the spinels in the dunite exhibit relatively high TiO₂ content compared to the spinels in the harzburgites (Figure 7). The composition of the spinels with relatively high Cr# in the dunite resembles that from the depleted harzburgite and all of these samples plot within fore-arc peridotites field (Figure 5).

The calculated forsterite content of olivines

(datas from Bilici, 2015) in the harzburgite and the dunite samples from the Yesilova ophiolite range between 89.67-91.61 mol% and 88.80-91.89 mol%, respectively. According to the forsterite content (Fo) of the olivines versus the Cr# of the spinel in these peridotites, the harzburgites and some of the dunites plot in the "Olivine-Spinel Mantle Array" (OSMA). However, many dunite samples plot out of this array (Figure 6). Also, olivine-spinel pairs from both of the harzburgite and dunite samples show almost similar distribution with the Fo contents of the olivines and the Cr# values of the spinels.

The studied chromian spinels are plotted on a Cr#-TiO₂ wt% diagram (Figure 7). Although the Cr#-TiO₂ diagram provides a method with which to discriminate MOR from SSZ settings, there is

ambiguity while using the diagram because of the significant overlap between two fields, especially for Cr# values between 0.45 and 0.6. However, relatively high-Ti chromian spinels in the studied dunites show clear correlation through to the reaction field. In this diagram, using spinel compositions obtained from dunites and harzburgites that are considered to be petrogenetically linked and it is probable to form a reaction trend that defines the composition of the reacting melt (Pearce *et al.*, 2000). Interaction between a Ti-poor, depleted mantle peridotite and a Ti-rich melt will upgrade the Ti content of a peridotite. Reaction between residual mantle or harzburgite and MORB-like melt is characterised by a reaction trend towards a composition with relatively low Cr# and upgrade TiO₂ wt % values in the dunite (Figure 7).

The spinels in the studied harzburgite and

dunite carry relatively limited varieties of trace elements measurable by the laser ablation ICP-MS. In particular, Ni, Co and Zn are notably abundant in the spinels, and significant concentrations of Ga, Sc, Ni, Ti, Mn and V are also present in this mineral phase (Figure 8). According to the lithology, the spinel chemistry demonstrates significant differences in terms of some transition elements. In particular, Ni, V, Co, Zn and Ga concentrations of the spinels in the harzburgites higher than in the dunites. However, the Ti content of the spinels is the reverse of this situation (Figure 8).

Although, Rare Earth Elements (REE) contents of the chromian spinels are very low concentrations, chondrite and primitive mantle normalized values exhibit clear patterns (Figure 9). Chondrite normalized REE patterns for the spinels in the harzburgite exhibit significant LREE

Figure 5. Plots of Cr# [100Cr / (Cr + Al)] vs. Mg# [100 Mg / (Mg + Fe²⁺)] of chromian spinels of the peridotites from the Yeşilova ophiolite (modified after Dick and Bullen, 1984)

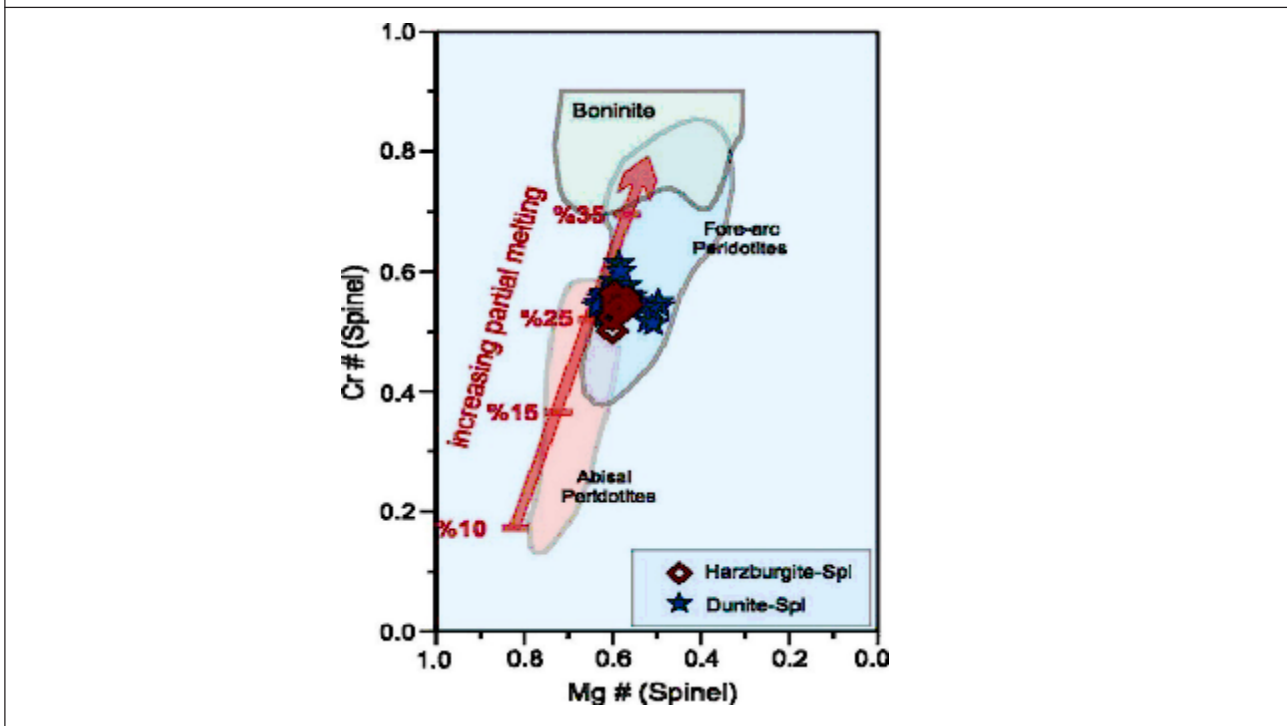
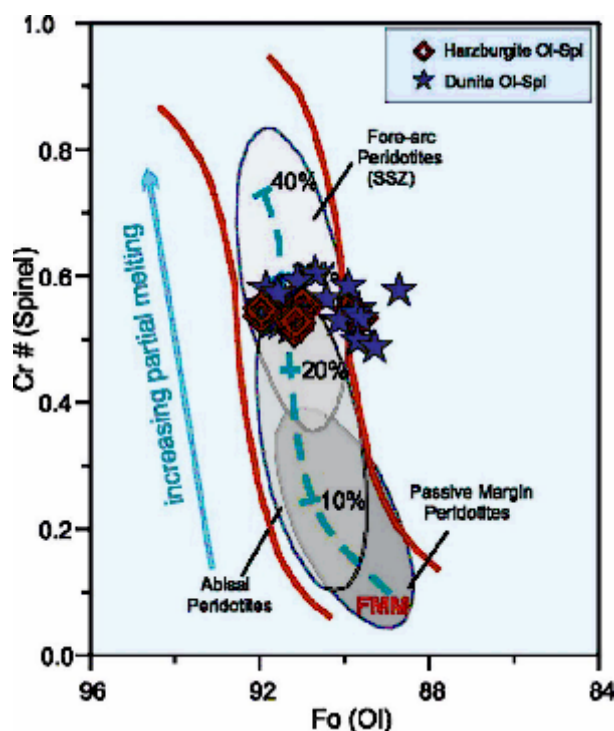


Figure 6: Plot of Cr# of spinel vs. Fo in olivine of the peridotites from the Yeşilova ophiolite in the olivine spinel mantle array (OSMA) diagram of Arai (1994). OSMA and melting trend are taken from Arai (1994). (The abyssal and supra-subduction zone (SSZ) peridotite fields are from Dick and Bullen, 1984, Ishii et al., 1992, Parkinson and Pearce, 1998 and Choi et al., 2008)



depletion, whereas the spinels in the dunite show flat patterns (Figure 9a-b). The distinct differences of the spinel concentrations between the harzburgite and the dunites, are graphically displayed by multi-element variation diagrams, in which the trace elements are arranged in order of increasing compatibility from left to right. The spinels in the harzburgites display a small Large Ion Lithophilic Elements (LILE) enrichment such as Rb, Ba, U, Th, Nb, Sr, and slight Y depletion (Figure 9c). However, LILE enrichment of the spinels in the dunite except for Ba concentration is a little more than in the harzburgite. Also, the spinels in the dunite exhibit slight Ti enrichment and low Y depletion (Figure 9d).

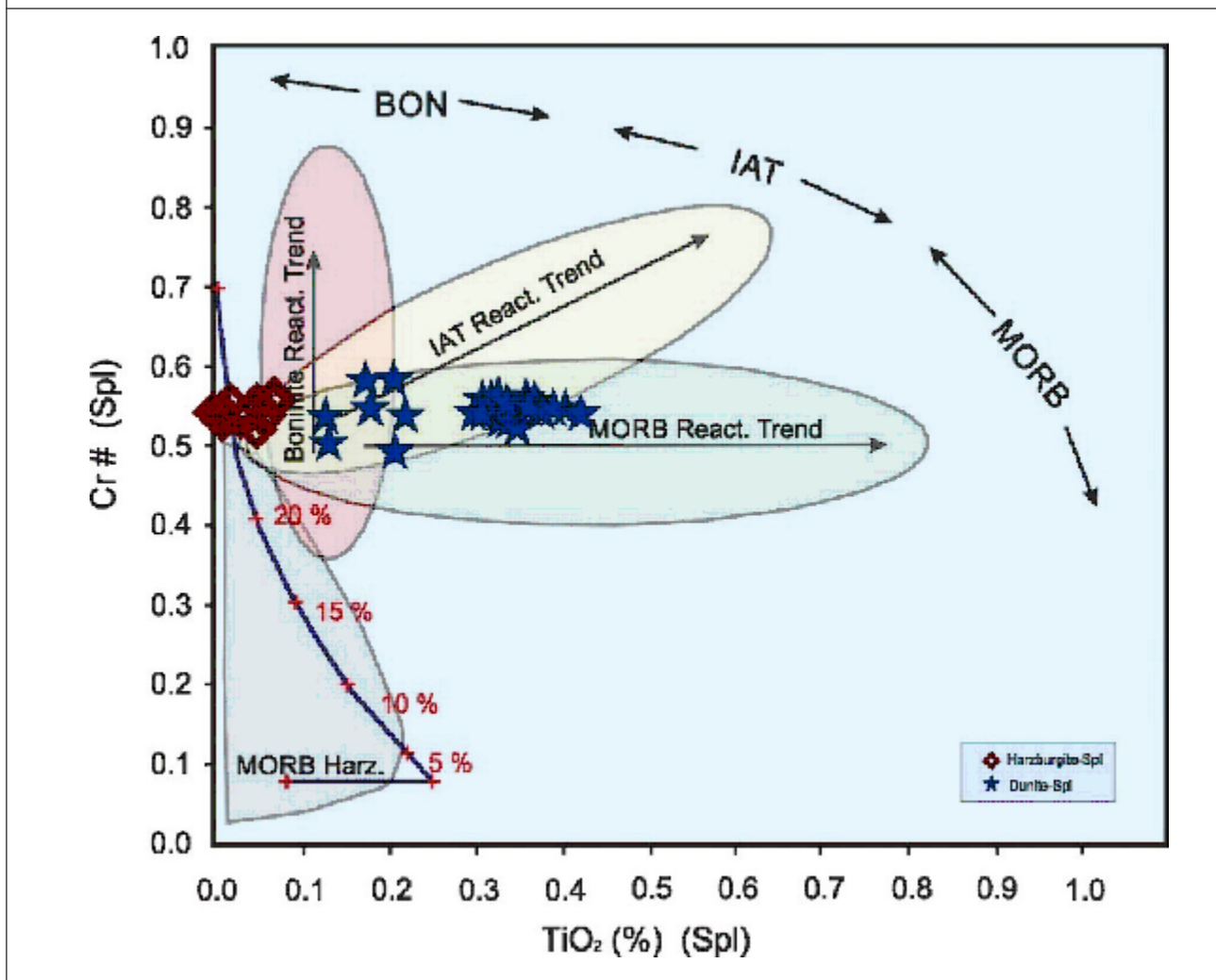
In summary, the significant differences in the spinels are observed from the harzburgite to the

dunite in chondrite normalized REE and primitive mantle normalized multi-element patterns.

DISCUSSION

The chemical properties of the studied chromian spinels show that partial melting processes and subsequent melt/rock interaction in the mantle section played a vital role during the evolution of these peridotites. The Cr# of chromian spinel can be utilized to examine the degree of partial melting experienced by means of chromian spinel-bearing peridotites (e.g., Dick and Bullen, 1984; Arai, 1994; Hellebrand *et al.*, 2001, 2002). The Cr#, Al and Ti contents of the chromian spinel are very useful to understand the characteristics of the parental melts of the spinels and the tectonic setting in which these melts were formed

Figure 7: Relationships Between TiO₂ Contents And Cr/(Cr + Al) Atomic Ratios Of Chromian Spinel In Harzburgite And Dunite From The Yesilova Ophiolite (After Pearce Et Al., 2000)



(e.g., Zhou *et al.*, 1996, Melcher *et al.*, 1997, Uysal *et al.*, 2007, Rollinson, 2008, Pagé and Barnes, 2009, González-Jiménez *et al.*, 2011; Zaccarini *et al.*, 2011; Zhou *et al.*, 2014).

The partial melting degree of the studied peridotite samples of the Yesilova ophiolite can be calculated by using their residual mineral compositions. The composition of primary spinels in upper mantle peridotites is generally highly illustrative. Actually, the Cr# reflects the relative degree of the partial melting (e.g., Arai, 1994; Hellebrand *et al.*, 2001). According to the Cr# of

the studied spinels, the highly depleted compositions of the harzburgite and dunite samples show that these rocks underwent moderate (~25 %) degrees of partial melting (Figure 5-7).

Considering the olivine-spinel pairs of the studied harzburgite and dunite, Fo contents of the olivine and the Cr# values of the spinel, most of the analyzed samples plot within the olivine-spinel mantle array (OSMA) described by Arai (1994), indicating that the Yesilova peridotites represent residual material remaining after partial

melting of the upper mantle (Figure 6).

Subduction-related ophiolites display a gradual geochemical affinity from MORB-like to Island Arc Tholeiite (IAT) and Boninite in the later phases of SSZ ophiolites (Dilek and Furnes, 2011). The varying degrees of Ti enrichment in peridotites result from the chromian spinels equilibrating with melts of different compositions (Kelemen *et al.*, 1995; Edwards and Malpas, 1995, 1996; Pearce *et al.*, 2000). Reaction between residual mantle and MORB-like melt is characterized by a reaction trend towards a composition with moderately low Cr# and higher TiO₂ wt % values. In this diagram, the point of intersection on the fertile mantle melt created by the studied peridotites demonstrates that the mantle is the product of an intermediate or relatively high degree (~25 %) of partial melting (Figure 7). The Cr# of the chromian spinels from the SSZ peridotites are characterized with much higher than abyssal peridotites, which indicates particularly higher degrees of partial melting in the SSZ peridotites (e.g., Arai, 1994; Gaetani and Grove, 1998). When the SSZ peridotites are influenced by later interaction with MORB-like melts, their spinels become enriched in TiO₂ without increasing in Cr# (Pearce *et al.*, 2000) (Figure 7).

Most of the ophiolites have met significant and different alteration processes that can potentially modify spinel composition. However, the chromian spinels is relatively resistant (especially core) to fluid-driven alteration and weathering relative to associated silicate minerals and thus may preserve many primary magmatic properties (e.g., Baumgartner *et al.*, 2013; Evans *et al.*, 2013; Zhou *et al.*, 2014). The major and trace element characteristics of the spinels reflect magmatic and metasomatic processes within the upper

mantle. For the spinels analyzed here, representing the compositional endmembers of the studied peridotites, Ga, Ni, V, Zn, Co contents decrease, and Sc, Ti and Mn contents increase from the harzburgite to the dunite with a little changing the Cr# of the spinels, suggesting a control by partial melting (Figure 8). The LREE-enriched patterns of the spinels in the dunite, on the other hand, clearly explain metasomatic enrichment of the highly incompatible elements within the upper mantle above a subduction zone (Figure 9b). Furthermore, the Nb, Ta and slight Ti enrichment of the spinels in the dunite and the Y depletion of the spinels in the harzburgite is associated with the reaction between harzburgite and reacted melt, subsequently forming the dunite body (Figure 9c-d).

CONCLUSION

This study reveals that the in-situ analysis of major and trace elements in the chromian spinels using EPMA and LA-ICP-MS may help to recognize fingerprints of petrogenetic interpretations between the harzburgite and dunite from the Yesilova ophiolite (SW Turkey). The mineral chemistry datas of the chromian spinels in the studied peridotites suggest that interaction between residual mantle and MORB-like melt has formed the dunite with relatively high-Ti and high-Al spinels in a supra-subduction zone. Consequently, we suggest that this MORB-like melt formed the dunite bodies with high-Al spinels compositions within the harzburgite is related to the subduction initiation or subsequently slab break off.

ACKNOWLEDGMENT

This paper presents part of the Ph.D. thesis of first author.

REFERENCES

1. Aldanmaz E, Meisel T, Çelik O F and Henjes-Kunst F (2012), "Osmium isotope systematics and highly siderophile element fractionation in spinel-peridotites from the Tethyan ophiolites in SW Turkey: implications for multi-stage evolution of oceanic upper mantle", *Chemical Geol.*, Vol. 294–295, 152–164.
2. Arai S (1992), "Chemistry of chromian spinel in volcanic rocks as a potential guide to magma chemistry", *Mineral. Magazine*, Vol. 56, pp. 173–184.
3. Arai S (1994), "Characterization of spinel peridotites by olivine–spinel compositional relationships: review and interpretation", *Chem. Geol.*, Vol.113, No. 3, 191–204.
4. Arai S, Kadoshima K and Morishita T (2006), "Widespread arc-related melting in the mantle section of the northern Oman ophiolite as inferred from detrital chromian spinels", *Journal of the Geological Society*, London, Vol. 163, pp. 869–79.
5. Arai S, Okamura H, Kadoshima K, Tanaka C, Suzuki K and Ishimaru S (2011), "Chemical characteristics of chromian spinel in plutonic rocks: Implications for deep magma processes and discrimination of tectonic setting", *Island Arc*, Vol. 20, pp. 125–137.
6. Barnes S J and Roeder P L (2001), "The range of spinel compositions in terrestrial mafic and ultramafic rocks", *J. Petrol.*, Vol. 42, No. 12, pp. 2279–2302.
7. Baumgartner R J, Zaccarini F, Garuti G and Thalhammer O A R (2013), "Mineralogical and geochemical investigation of layered chromitites from the Bracco–Gabbro complex, Ligurian ophiolite, Italy", *Contributions to Mineralogy and Petrology*, Vol.165, pp. 477-493.
8. Bilici Ö (2015), "Comparative Investigation of Kop (Erzurum-Erzincan-Bayburt), Ulaş (Sivas) and Yesilova (Burdur) Ultramafics and Chromitites in terms of Mineralogical, Petrological and Geodynamical Aspects", (In Turkish) PhD Thesis, Karadeniz Technical University, Trabzon, Turkey, p. 313.
9. Choi S H, Shervais J W and Mukasa S B (2008), "Supra-subduction and abyssal mantle peridotites of the Coast Range ophiolite, California". *Contrib. Mineral. Petrol.*, pp. 156, 551-576.
10. Dare S A S, Pearce J A, McDonald I and Styles M T (2009), "Tectonic discrimination of peridotites using fO₂ – Cr and Ga-Ti-Fe³⁺ systematic in chrome-spinel". *Chemical Geol.*, Vol. 261, pp. 199-216.
11. Dick H J B and Bullen T (1984), "Chromian spinel as a petrogenetic indicator in abyssal and alpine-type peridotites and spatially associated lavas". *Contrib. Mineral. Petrol.*, Vol.86, pp. 54–76.
12. Dilek Y and Furnes H (2011), "Ophiolite genesis and global tectonics: geochemical and tectonic fingerprinting of ancient oceanic lithosphere". *Geol. Soc. Am. Bulletin*, Vol.123, pp. 387–411.
13. Döyen A (1995), "Mineralogical, petrographical and geochemical studies of the chromite ore deposits in Yesilova (Burdur) district". PhD thesis, Selçuk University, Graduate School of Natural and Applied Sciences, p. 118.

14. Döyen A, Çömlekçiler F and Koçak K (2014), "Stratigraphic Features of the Yesilova Ophiolite, Burdur, South-Western Turkey", Springer Geology, Strati 2013, 493-498.
15. Edwards S J and Malpas J (1995), "Multiple Origins for Mantle Harzburgite; Examples from the Lewis Hills, Bay of Islands Ophiolite, Newfoundland". *Canadian Journal of Earth Sci.*, Vol. 32, pp. 1046-1057.
16. Edwards S J and Malpas J (1996), "Melt-peridotite interactions in shallow mantle at the East Pacific Rise: evidence from ODP Site 895 (Hess Deep)". *Min. Magazine*, Vol. 60, pp. 191- 206.
17. Edwards S J, Pearce J A and Freeman J (2000), "New insights concerning the influence of water during the formation of podiform chromitite": In; Dilek Y, Moores E M, Nicolas A and Elthon D (Eds.), "Ophiolites and Oceanic Crust: New Insights from Field Studies and the Ocean Drilling Program", *Geological Society of America*, Special Paper, Vol. 349, pp. 139–147.
18. Evans K A, Powell R and Frost B R (2013), "Using equilibrium thermodynamics in the study of metasomatic alteration, illustrated by an application to serpentinites". *Lithos*, Vol.168–169, pp. 67–84.
19. Flower M F J and Dilek Y (2003), "Arc-trench rollback and forearc accretion: 1. A collision-induced mantle flow model for Tethyan ophiolites" in Dilek Y and Robinson P T (Eds). "Ophiolites in Earth history". *Geological Society (London) Special Publication*, Vol. 218, pp. 21– 41.
20. Gaetani G A and Grove T L (1998), "The influence of water on melting of mantle peridotite". *Contrib. Mineral. Petrol.*, Vol.131, pp. 323–346.
21. Gonzalez–Jimenez J M, Proenza J A, Gervilla F, Melgarejo J C, Blanco–Moreno J A, Ruiz–Sanchez R and Griffin W L (2011), "High–Cr and High–Al Chromitites from The Sagua de Tanamo District, Mayari–Cristal Ophiolitic Massif (Eastern Cuba): Constraints on Their Origin from Mineralogy and Geochemistry of Chromian Spinel and Platinum–Group Elements", *Lithos*, p. 2396.
22. González-Jiménez J M, Marchesi C, Griffin W L, Gutiérrez-Narbona R, Lorand J P, O'Reilly S Y, Garrido C J, Gervilla F, Pearson N J and Hidas K (2013), "Transfer of Os isotopic signatures from peridotite to chromitite in the subcontinental mantle: Insights from in situ analysis of platinum-group and base-metal minerals (Ojén peridotite massif, southern Spain)". *Lithos*, Vol. 164, pp. 74–85.
23. González-Jiménez J M, Griffin W L, Proenza J A, Gervilla F, O'Reilly S Y, Akbulut M, Pearson N J and Arai S (2014), "Chromitites in ophiolites: How, where, when, why? Part II. The crystallization of chromitites". *Lithos*, Vol.189, pp. 140-158.
24. González-Jiménez J M, Locmelis M, Belousova E, Griffin W L, Gervilla F, Kerestedjian T N, O'Reilly S Y, Pearson N J and Sergeeva I (2015), "Genesis and tectonic implications of podiform chromitites in the metamorphosed Ultramafic Massif of Dobromirski (Bulgaria)". *Gondwana Res.*, Vol.27, No. 2, pp. 555–574.
25. Hellebrand E, Snow J E, Dick H J B and

- Hofmann A W (2001), "Coupled major and trace elements as indicators of the extent of melting in mid-ocean-ridge peridotites". *Nature*, Vol.410, pp. 677–681.
26. Hellebrand E, Snow J E, Hoppe P and Hofmann A W (2002), "Garnet-field melting and late-stage refertilization in residual abyssal peridotites from the Central Indian Ridge". *Journal of Petrol.*, Vol.43, pp. 2305–2398.
27. Hill R and Roeder P (1974), "The crystallization of spinel from basaltic liquid as a function of oxygen fugacity". *Journal of Geol.*, Vol. 82, No. 6, pp. 709–729.
28. Irvine T N (1965), "Chromian spinel as a petrogenetic indicator, Part 1. Theory". *Can. J. Earth Sci.* Vol.2, pp. 648–672.
29. Irvine T N (1967), "Chromian spinel as a petrogenetic indicator. Part 2. Petrologic applications". *Can. J. Earth Sci.*, Vol. 4, pp. 71–103.
30. Jackson E D (1969), "Chemical variation in coexisting chromite and olivine in chromitite zones of the Stillwater Complex". *Econ. Geol. Monogr.*, Vol.4, pp. 41–71.
31. Kamenetsky V S, Crawford A J and Meffre S (2001), "Factors controlling chemistry of magmatic spinel: an empirical study of associated olivine, Cr-spinel and melt inclusions from primitive rocks". *J. Petrol.*, Vol.42, No. 4, pp. 655–671.
32. Kelemen P B, Shimizu N and Salters V J M (1995), "Extraction of mid-ocean ridge basalt from the upwelling mantle by focused flow of melt in dunite channels". *Nature*, Vol. 375, pp. 747–753.
33. Maurel C and Maurel P (1982), "Etude expérimentale de la distribution de l'aluminium entre bain silicaté basique et spinelle chromifère. Implications pétrogénétiques: teneur en chrome des spinelles". *Bull. Mineral.*, Vol. 105, pp. 197–202.
34. Melcher F, Grum W, Simon G, Thalhammer T V and Stumpfl F E (1997), "Petrogenesis of the ophiolitic giant chromite deposits of Kempirsai, Kazakhstan: a study of solid and fluid inclusions in chromite". *J. Petrol.*, Vol. 38, pp. 1419–1438.
35. Moghadam H S, Khedr Z M, Arai S, Robert J S, Ghorbani G, Tamura A, Ottley C J (2015), "Arc-related harzburgite–dunite–chromitite complexes in the mantle section of the Sabzevar ophiolite, Iran: A model for formation of podiform chromitites". *Gondwana Research*, Vol. 27, pp. 575–593.
36. MTA (2002), "1:500,000 scale Geology Map of Turkey". *General Directorate of Mineral Research and Exploration*, Ankara, Turkey.
37. Okay I A and Tüysüz O (1999), "Tethyan Sutures of Northern Turkey". *Geological Society of London*, Special Publication, Vol. 156, pp. 475–515.
38. Pagé P and Barnes S J (2009), "Using trace elements in chromites to constrain the origin of podiform chromitites in the Thetford Mines ophiolite, Québec". *Canada. Econ. Geol.*, Vol. 104 (7), pp. 997–1018.
39. Parkinson I J and Pearce J A (1998), "Peridotites from the Izu–Bonin–Mariana forearc (ODP Leg 125): evidence for mantle melting and melt–mantle interaction in a

- supra-subduction zone setting". *Jour. Petrol.*, Vol. 39, pp. 1577–1618.
40. Pearce J A, Barker P F, Edwards S J, Parkinson I J, Leat P T (2000), "Geochemical and tectonic significance of peridotites from the South Sandwich arc-basin system, South Atlantic". *Contrib. Mineral Petrol.*, Vol.139, 36–53.
 41. Roeder P L (1994), "Chromite; from the fiery rain of chondrules to the Kilauea Iki lava lake". *Can. Mineral.*, Vol.32 (4), pp. 729–746.
 42. Rollinson P (2008), "The geochemistry of mantle chromitites from the northern part of the Oman ophiolite: inferred parental melt compositions". *Contrib. Mineralogy and Petrology*, Vol.156, pp. 273–288.
 43. Sack R O and Ghiorso M S (1991), "Chromian spinels as petrogenetic indicators; thermodynamics and petrological applications". *Am. Mineral.*, Vol. 76 (5-6), pp. 827–847.
 44. Sarp H (1976), "Etude Geologique et Petrographique du cortage Ophilitique de la Region Situee au Nord-Qest de Yesilova (Burdur-Turquie)". Ph.D. Thesis, Univ. Geneve, Italy.
 45. Seyler M, Lorand J P, Dick H J B and Drouin M (2007), "Pervasive melt percolation reactions in ultra-depleted refractory harzburgites at the Mid-Atlantic Ridge, 15–20 N: ODP Hole 1274A". *Contrib. Mineral. Petrol.*, Vol.153, pp. 303–319.
 46. Shi R, Griffin W L, O'Reilly S Y, Huange Q, Zhang X, Liu D, Zhi X, Xia Q and Ding L (2012), "Melt/Mantle Mixing Produces Podiform Chromite Deposits in Ophiolites: Implications of Re–Os Systematics in the Dongqiao Neo-Tethyan Ophiolite, Northern Tibet". *Gondwana Research*, Vol. 21, pp. 194–206.
 47. Sun S S and McDonough W F (1989), "Chemical and isotopic systematics of oceanic basalts: implications for mantle composition and processes". In: Saunders A D and Norry M J (Eds.), "Magmatism in the Ocean Basins". *Geological Society Special Publication*, Vol. 42, pp. 313– 345.
 48. Uysal I, Kaliwoda M, Karsli O, Tarkian M, Sadiklar M B and Ottley C J (2007), "Compositional variations as a result of partial melting and melt-peridotite interaction in an upper mantle section from the Ortaca area, southwestern Turkey". *Can. Mineral.*, Vol. 45, pp. 1471–1493.
 49. Uysal I, Ersoy E Y, Karsli O, Dilek Y, Sadiklar M B, Ottley C J, Tiepolo M and Meisel T (2012), "Coexistence of abyssal and ultra-depleted SSZ type mantle peridotites in a Neo-Tethyan Ophiolite in SW Turkey: Constraints from mineral composition, whole-rock geochemistry (major–trace–REE–PGE), and Re–Os isotope systematics". *Lithos*, Vol. 132–133, pp. 50–69.
 50. Uysal I, Dündar A P, Ersoy E Y, Dilek Y, Saka S, Zaccarini F, Escayola M and Karslı O (2014), "Geochemical make-up of oceanic peridotites from NW Turkey and the multi-stage melting history of the Tethyan upper mantle". *Miner. Petrol.*, Vol. 108, pp. 49–69.
 51. Zaccarini F, Garuti G, Proenza J A, Campos L, Thalhammer O A R, Aiglsperger T and Lewis J (2011), "Chromite and platinum-group-elements mineralization in the Santa Elena ophiolitic ultramafic nappe (Costa

- Rica): geodynamic implications". *Geol. Acta*, Vol. 9 (3–4), pp. 407– 423.
52. Zhou M F, Robinson P T, Malpas J and Li Z (1996), "Podiform Chromitites in The Luobusa Ophiolite (Southern Tibet), Implications for Melt-rock Interaction and Chromite Segregation in The Upper Mantle". *Journal of Petrol.*, Vol. 37, pp. 3–21.
53. Zhou M F, Robinson, P T, Su B X, Gao J F, Li J W, Yang J S and Malpas J (2014), "Compositions of Chromite, Associated Minerals, and Parental Magmas of Podiform Chromite Deposits: the Role of Slab Contamination of Asthenospheric Melts in Suprasubduction Zone Environments". *Gondwana Research*, Vol. 26, pp. 262-283.



International Journal of Geology and Earth Sciences

Hyderabad, INDIA. Ph: +91-09441351700, 09059645577

E-mail: editorijges@gmail.com or editor@ijges.com

Website: www.ijges.com

